Available online at www.sciencedirect.com

ScienceDirect

Journal of the Franklin Institute 357 (2020) 8137–8155

www.elsevier.com/locate/jfranklin

Solving time-varying linear inequalities by finite-time convergent zeroing neural networks

Yuejie Zeng[a], Lin Xiao[b,*], Kenli Li[a], Qiuyue Zuo[a], Keqin Li[a]

[a] *College of Information Science and Engineering, Hunan University, Changsha 410082, China*

[b] *Hunan Provincial Key Laboratory of Intelligent Computing and Language Information Processing, Hunan Normal University, Changsha 410081, China*

Received 23 June 2019; received in revised form 25 February 2020; accepted 3 June 2020

Available online 13 June 2020

Abstract

In this paper, to solve time-varying linear inequalities much faster, on basis of zeroing neural network (ZNN), two finite-time convergent ZNN (FTCZNN) models are proposed by exploiting two novel nonlinear activation functions (AFs). The first FTCZNN model is established by using the sign-bi-power AF which is termed as FTCZNN-S for presentation convenience. The second one is established by amending the sign-bi-power AF through adding a linear term, and called FTCZNN-SL. Compared with existing ZNN models for time-varying linear inequalities, the proposed two FTCZNN models possess prominent finite-time convergence performance. In addition, theoretical analysis is given to estimate the finite-time convergence upper bounds of those two FTCZNN models. Numerical comparative results ulteriorly validate the effectiveness and dominance of two FTCZNN models for finding the solution of time-varying linear inequalities.

1. Introduction

Solving inequalities is widely regarded as a fundamental problem in scientific research and engineering fields [1–5]. For example, Zhang [1] proposed a primal-dual neural network based on linear variational inequality (LVI), which allows the motion control scheme of redundant

* Corresponding author.

E-mail address: xiaolin860728@163.com (L. Xiao).

https://doi.org/10.1016/j.jfranklin.2020.06.004

manipulators to consider the physical limit of joints. In [2], the robust filtering problem based on Hopfield neural network was studied, in which the filter design is realized by solving linear matrix inequality. In [3], a modified upper bound of the globally convergent discrete time recurrent neural network for solving linear inequalities was proposed without the need for the solution set of the original linear systems. Hao and Zhao [4] presented the static output-feedback stabilisation and controller design method of discrete networked control system, where all the results were expressed by linear matrix inequalities (LMIs) and verified by Matlab LMI toolbox. Su et al. [5] derived a novel method based on cellular neural networks to eliminate image noise by using the characteristics of linear inequality matrix. Therefore, to some degree, solving linear inequalities possesses more wide applications, as compared to linear and nonlinear equations solving.

With the high-speed development of various computational methods [6], considerable efforts have been made for finding solutions to linear inequalities. For instance, Lin et al. [7] developed a novel approach to solve linear inequalities based on a matrix oriented gradient. In [8], Guo and Zhang proposed a new neural network model to solve linear matrix inequalities. In [9], a new explicit bound on the ratio of absolute error to the approximate solution of linear inequalities was proposed, and this bound generalizes the notion of norms for nonsingular matrix inverses. Because of the limitation of Matlab toolbox, we often solve time-varying linear inequalities by solving ordinary differential equations. On the one hand, we can convert time-varying linear inequalities into an optimization problem (such as a linear program) and then solve them by using classic methods, like simplex method and punishment method. These methods often require matrix operations, so they cannot be effectively applied to large-scale solving problems.

In recent decades, because of the hardware realization and the parallel-distributed nature, neural network has been proposed, developed, and studied in various areas [10–14]. A two-layer recurrent neural network [10] with low complexity is presented to solve non-smooth convex optimization problems. In [11], a sub-gradient recurrent neural network with finite convergence time period for solving two-layer linear programming problems is put forward. Furthermore, different from the conventional serial iterative algorithms, neural networks can be realized by hardware circuit and thus has attracted the attention of scholars. In [15], a novel neural network model has been presented to solve a class of linear variational inequalities with linear constraints. In [16,17], projection neural networks have been established to solve linear variational inequalities and related quadratic programming problems. The identification of discrete-time nonlinear systems based on recurrent neural networks was presented and studied in [18,19]. Owing to the thorough research of neural networks, recurrent neural networks [20,21] are regarded as effective approaches to solve linear and nonlinear time-varying inequalities.

Zeroing neural network (ZNN), which originates from Hopfield neural network, is a classification of recurrent neural network (RNN). Before the ZNN model is proposed, gradient neural network (GNN) is generally adopted to solve inequalities and equations. However, for time-varying cases, error function of GNN model can not converge to zero. To solve this problem, ZNN is designed and studied. It effectively takes advantage of the time derivative information and expedites the convergence rate of error function. In [22], the comparison between ZNN and GNN was given and simulation results demonstrated the better performance of ZNN. Meanwhile, ZNN is widely used in various solving process of equations and inequalities, such as matrix-vector inequalities solving [23]. A novel discrete-time ZNN model [24] is proposed for matrix inversion. In [25], the ZNN model is used to solve the sys-

Table 1
The main differences and novelties of the FTCZNN models from other models published in [36–40].

Item	Problem	Activation function	Finite Convergence	Upper bound
[36]	Equation and inequalities	Power-sum	Infinite	-
[37]	Quadratic programming	Linear	Infinite	-
[38]	Matrix Inversion	Sign-bi-power	Finite	Conservative
[39]	Darzin inverse	Nonlinear function	Infinite	-
[40]	Sylverster equation	Sign-bi-power	Finite	Conservative
This paper	Linear Inequalities	Improved sign-bi-power	Finite (accelerated)	Less conservative

tems of time-varying linear inequalities. Xiao [26] proposed a finite-time ZNN model to find time-varying matrix square root. In [27,28], three different activation functions (AFs) are presented to activate ZNN for solving Sylvester equation, and the finite-time convergence performance [29] can even be achieved when using the sign-bi-power AF. In addition, using a novel ZNN model can achieve finite-time convergence for solving equations in [30,31].

Furthermore, finite-time control and convergence properties play a more and more irreplaceable role in improving tracking accuracy and performance, which provide motivation for us to study the finite time convergence when solving time-varying inequalities. For instance, in [32], finite-time control provides the possibility of high quality industrial robot control. In [33], based on finite time control, a high performance adaptive fuzzy control filter is implemented. Zou et al. [34] realized precise attitude tracking control of spacecraft according to finite time control. Furthermore, the spacecraft achieved accurate formation control over obstacles in [35]. As we know, time-varying equations have been well solved by zeroing neural networks, and some of these can even achieve finite-time convergence. However, in terms of solving time-varying inequalities, the current neural networks can only make its error function exponentially converge to zero, but cannot achieve finite time convergence. Hence, the solution to time-varying inequality may not be extended to practical applications because of high restriction on computation time.

Aiming at the superiority of ZNN in solving various time-varying inequality problems, in this paper, two finite-time convergent ZNN (FTCZNN) models are proposed and studied to find the solution to the time-varying linear inequalities. The first FTCZNN model, which is termed as FTCZNN-S, is an improvement on the conventional ZNN model by applying the sign-bi-power AF. The second one is developed by amending the sign-bi-power AF through adding a linear term, and called FTCZNN-SL. The design method of two FTCZNN models is based on a lower unbounded error function. Therefore, for any initial state inside the initial solution set of time-varying linear inequalities, the error functions of two FTCZNN models are always equal to the initial errors corresponding to any initial state (lower bound). Meanwhile, when the initial state is not inside the initial solution set, the convergence property of two FTCZNN models is still very superior, and finite-time convergence is even achieved. That is to say, both FTCZNN models are able to obtain exact time-varying solutions. In order to further show the excellence of the FTCZNN models, we have compared our work with some of the recent literatures (i.e., [36–40]) on solving various problems by using zeroing neural networks, and the comparative results have been listed in Table 1. From this table, it can be concluded that our work is not only efficient on solving time-varying problems, but also has faster finite-time convergence speed. In addition, this is the first work to solve time-varying linear equalities using zeroing neural network to realize the finite-time convergence.

The remainder of this work is divided into four sections. Section 2 introduces the design method of ZNN, and two FTCZNN models are proposed by adopting two novel nonlinear AFs. Section 3 substantiates the global convergence and finite-time convergence of two FTCZNN models. Section 4 shows the simulation verification of two FTCZNN models as well as comparisons between models proposed in this paper and in other related published works. In Section 5, the conclusion of this work is given. Before ending this section, the major contributions of this work are listed as below.

(1) As great improvements to the conventional ZNN model with infinite-time convergence, two FTCZNN models are proposed and proved to be capable of finite-time convergence for time-varying linear inequalities. This naturally becomes the most significant highlight of this work.
(2) Two different nonlinear AFs are presented to establish FTCZNN models, which are based on the vector-valued error functions, instead of the traditional scalar-valued energy functions.
(3) Through rigorous theoretical analysis of these two FTCZNN models, their excellent finite-time convergence property is guaranteed. In addition, the upper bounds for two FTCZNN models are theoretically calculated by using Lyapunov stability theory, when initial states are outside the initial solution set of time-varying linear inequalities.
(4) Two examples are given to verify the superiority of two FTZCNN models in convergence performance to existing ZNN models activated by other AFs.

2. FTCZNN models

In this part, we study the solution to time-varying linear inequalities with the following form:

$$A(t)x(t) \leq b(t), \tag{1}$$

where t denotes time, $A(t) \in \mathbb{R}^{n\times n}$ and $b(t) \in \mathbb{R}^n$ are given time-varying coefficients. The solution set is defined as $\Omega(t) = \{x(t)|x(t) \in \mathbb{R}^n \text{ solves } (1)\}$. The aim of this work is to find the unknown $x(t) \in \mathbb{R}^n$ within finite time such that the above time-varying inequality system (1) always holds true. For the sake of presentation, we define the residual error as

$$g(t) = A(t)x(t) - b(t) \in \mathbb{R}^n, \tag{2}$$

where $g(t) = [g_1(t), g_2(t), \cdots, g_n(t)]^{\mathrm{T}}$. Obviously, if $g(t) \leq 0$, the resultant $x(t)$ is what we want to solve for. In this section, for establishing two FTCZNN models, the original ZNN model for time-varying linear inequalities is first given. Then, by introducing new activation functions, two FTCZNN models are proposed to solve time-varying linear inequalities.

2.1. ZNN model

In order to facilitate the observation of the whole process of solving linear inequalities, we first define a vector-valued error function:

$$E(t) = [e_1(t), e_2(t), \ldots, e_n(t)]^{\mathrm{T}}, \tag{3}$$

with $e_i(t) = g_i(t),\ i = 1, 2, \ldots, n.$

Second, a new differential formula is constructed to make error function (3) converge to zero. Different from previous differential formula for error function (3), the novel method can exploit different activation functions to shorten the convergence time. The new differential formula for the error function (3) is presented as follows:

$$\frac{\mathrm{d}E(t)}{\mathrm{d}t} = -\epsilon \mathrm{STP}(E(0)) \diamondsuit \Psi(E(t)), \tag{4}$$

where ϵ is a positive parameter, $\Psi(\cdot) : \mathbb{R}^n \to \mathbb{R}^n$ is a set of activation functions, and $\mathrm{STP}(\cdot) : \mathbb{R}^n \to \mathbb{R}^n$ stands for a set of step functions with each element defined as

$$\mathrm{stp}(a) = \begin{cases} 1, & a > 0; \\ 0, & a \leq 0. \end{cases} \tag{5}$$

Besides, the operator $\diamondsuit$ is defined as

$$c \diamondsuit d = \begin{bmatrix} c_1 d_1 \\ c_2 d_2 \\ \vdots \\ c_n d_n \end{bmatrix}. \tag{6}$$

Thus, we can obtain the dynamic equation of the ZNN model for solving time-varying linear inequalities:

$$A(t)\dot{x}(t) = -\epsilon \mathrm{STP}(A(0)x(0) - b(0)) \diamondsuit \Psi(A(t)x(t) - b(t)) - \dot{A}(t)x(t) + \dot{b}(t). \tag{7}$$

It is worth pointing out that the above ZNN model (7) has been proved to be globally convergent when $\Psi(\cdot)$ satisfies the monotonicity and parity. In the following part, two finite-time convergent AFs are explored to shorten the convergence time of ZNN model (7). This is the first application to this ZNN model for solving time-varying linear inequalities.

2.2. Novel activation functions

In the past years, the following AFs are widely applied in ZNN models: (1) the linear activation function:

$$\Psi(x) = x; \tag{8}$$

(2) the power activation function:

$$\Psi(x) = x^p, p \geq 3; \tag{9}$$

(3) the bipolar-sigmoid activation function:

$$\Psi(x) = \frac{1 + \exp(-p)}{1 - \exp(-p)} \frac{1 - \exp(-px)}{1 + \exp(-px)}, p > 2; \tag{10}$$

(4) the power-sigmoid activation function:

$$\Psi(x) = \frac{1}{2} x^{p_1} + \frac{1 + \exp(-p_2)}{1 - \exp(-p_2)} \frac{1 - \exp(-p_2 x)}{1 + \exp(-p_2 x)}, p_1 \geq 3, p_2 > 2. \tag{11}$$

However, the above mentioned AFs cannot make ZNN model (7) to achieve finite-time convergence in solving time-varying linear inequalities. For equality problems solving, Li et al. [27,28] proposed a new nonlinear AF named the sign-bi-power activation function, which can

accelerate ZNN to finite-time convergence. Inspired by this point, in order to make ZNN model (7) converge to the solution of time-varying linear inequalities within finite-time, the sign-bi-power AF is first applied to this model. Then, to solve time-varying linear inequalities much faster, a modified sign-bi-power AF is further applied to accelerate the convergence speed of ZNN model (7).

Specifically, the sign-bi-power AF is given as follows:

$$\Psi_1(x) = \frac{1}{2}|x|^r \text{sign}(x) + \frac{1}{2}|x|^{\frac{1}{r}} \text{sign}(x), \tag{12}$$

where $0 < r < 1$ and $\text{sign}(\cdot)$ is defined as:

$$\text{sign}(x) = \begin{cases} 1, & \text{if } x > 0; \\ 0, & \text{if } x = 0; \\ -1, & \text{if } x < 0. \end{cases} \tag{13}$$

In order to improve the convergence speed, on basis of sign-bi-power AF (12), an improved sign-bi-power AF is designed by adding a linear term, and is presented as below:

$$\Psi_2(x) = \frac{1}{2}|x|^r \text{sign}(x) + \frac{1}{2}x + \frac{1}{2}|x|^{\frac{1}{r}} \text{sign}(x). \tag{14}$$

Remark 1. Generally speaking, chattering phenomenon appears when discontinuous functions (e.g., sign function) are applied in nonlinear systems. In this work, we have explored two nonlinear activation functions (including the sign term) to accelerate the convergence speed of ZNN model (7). For avoiding chattering phenomenon generated by the sign function, we do not directly use the sign function as activation functions to accelerate the convergence speed of ZNN model (7). In contrast, we have explored two sign-bi-power functions (including the sign term) as activation functions. Obviously, these two sign-bi-power functions are continuous ones. Therefore, chattering phenomenon is avoided by using two continuous sign-bi-power functions. The continuity proofs of the two activation functions are provided as below.

The sign-bi-power AF (12) can be rewritten as:

$$\Psi_1(x) = \begin{cases} \frac{1}{2}x^r + \frac{1}{2}x^{\frac{1}{r}}, & x > 0; \\ 0, & x = 0; \\ \frac{1}{2}(-x)^r + \frac{1}{2}(-x)^{\frac{1}{r}}, & x < 0. \end{cases} \tag{15}$$

Obviously, when $x > 0$ and $x < 0$, the expressions of the sign-bi-power AF are continuous, so we only need to prove the continuity of the sign-bi-power AF (12) at the point $x = 0$. Because $\Psi_1(0) = \lim_{x\to 0^-}\left((-x)^r/2 + (-x)^{\frac{1}{r}}/2\right) = \lim_{x\to 0^+}\left(x^r/2 + x^{\frac{1}{r}}/2\right) = 0$, we can conclude that the sign-bi-power AF (12) is continuous at the point $x = 0$. In summary, the sign-bi-power AF (12) is a continuous function. In the same way, we can prove that the improved sign-bi-power function (14) is also continuous.

2.3. FTCZNN models

In this section, by injecting AFs (12) and (14) into ZNN model (7), we can obtain the corresponding two FTCZNN models to solve time-varying linear inequalities. Their simplified design processes are presented as below.

(1) *FTCZNN-S model*: Similar to the design process of ZNN model (7), the error function is first defined as $E(t)$. Then, the differential formula for this error function is given as

$$\dot{E}(t) = -\epsilon \text{STP}(E(0)) \diamondsuit \Psi_1(E(t)), \tag{16}$$

where $\Psi_1(\cdot)$ denotes the sign-bi-power AF (12), $E(0)$ denotes the initial error of $E(t)$ at $t = 0$, STP$(\cdot)$ and $\diamondsuit$ are defined as before.

At last, expanding the differential formula (16) by substituting $E(t)$, the dynamic equation corresponding to the FTCZNN-S model is formed by

$$\begin{aligned} A(t)\dot{x}(t) = &-\epsilon \mathrm{STP}(A(0)x(0) - b(0)) \diamondsuit \Psi_1(A(t)x(t) - b(t)) \\ &-\dot{A}(t)x(t) + \dot{b}(t). \end{aligned} \tag{17}$$

(2) *FTCZNN-SL model*: On the basis of FTCZNN-S model (17), AF is changed to the improved sign-bi-power AF (14). Then, the differential formula for the error function is obtained as follows:

$$\dot{E}(t) = -\epsilon \mathrm{STP}(E(0)) \diamondsuit \Psi_2(E(t)), \tag{18}$$

and the corresponding FTCZNN-SL model is formed by

$$\begin{aligned} A(t)\dot{x}(t) = &-\epsilon \mathrm{STP}(A(0)x(0) - b(0)) \diamondsuit \Psi_2(A(t)x(t) - b(t)) \\ &-\dot{A}(t)x(t) + \dot{b}(t). \end{aligned} \tag{19}$$

3. Theoretical analysis

In this part, we will analyze the global convergence property of FTCZNN-S model (17) and FTCZNN-SL model (19), and then discuss their finite-time convergence property further.

3.1. Global convergence

It has been proved that ZNN model (7) can achieve the global convergence, provided that nonlinear AFs are monotonically increasing odd functions. According to this point, in order to verify the global convergence of FTCZNN-S (17) and FTCZNN-SL (19), it is necessary for us to prove the parity of AFs (12) and (14) at first.

Theorem 1. *Given smoothly time-varying coefficient matrix $A(t) \in \mathbb{R}^{n\times n}$ and vector $b(t) \in \mathbb{R}^n$, FTCZNN-S model (17) and FTCZNN-SL model (19) are globally convergent. That is to say, no matter what the initial states $x(0)$ are, state vectors $x(t)$ are correspondingly convergent to the theoretical solution set $\Omega(t)$ of Eq. (1).*

Proof. First, let us review the definitions of AFs (12) and (14), from which we can get

$$\begin{aligned} \Psi_1(-x) &= \frac{1}{2}|-x|^r \mathrm{sign}(-x) + \frac{1}{2}|-x|^{\frac{1}{r}} \mathrm{sign}(-x) \\ &= -\frac{1}{2}|x|^r \mathrm{sign}(x) - \frac{1}{2}|x|^{\frac{1}{r}} \mathrm{sign}(x) \\ &= -\Psi_1(x). \end{aligned} \tag{20}$$

$$\begin{aligned} \Psi_2(-x) &= \frac{1}{2}|-x|^r \mathrm{sign}(-x) - \frac{1}{2}x + \frac{1}{2}|-x|^{\frac{1}{r}} \mathrm{sign}(-x) \\ &= -\frac{1}{2}|x|^r \mathrm{sign}(x) - \frac{1}{2}x - \frac{1}{2}|x|^{\frac{1}{r}} \mathrm{sign}(x) \\ &= -\Psi_2(x). \end{aligned} \tag{21}$$

Hence, we can conclude that AFs (12) and (14) satisfy the parity. On the other hand, AFs (12) and (14) are monotonically increasing. That is to say, such two finite-time convergent AFs are monotonically increasing odd functions. Thus, for proving the global convergence of FTCZNN-S model (17) and FTCZNN-SL model (19) in a unified manner, we only need consider the following formula:

$$\dot{E}(t) = -\epsilon \mathrm{STP}(E(0)) \diamondsuit \Psi(E(t)),$$

because FTCZNN-S model (17) and FTCZNN-SL model (19) can be equivalently derived from this design formula by choosing different AFs.

Next, we only need equivalently to prove the global convergence of the above design formula. Considering the definition of STP(·), the proof is divided into two cases according to whether initial state $x(0) \in \mathbb{R}^n$ is inside of initial solution set $\Omega(0)$ or not.

Case I If initial state $x(0) \in \mathbb{R}^n$ is inside of the initial solution set $\Omega(0)$, we can obtain $g(0) \leq 0$. That is to say, $E(0) \leq 0$, which means $\mathrm{STP}(E(0)) = 0$. So, $\dot{E}(t) = -\epsilon \mathrm{STP}(E(0)) \diamondsuit \Psi(E(t)) = 0$.

Therefore, no matter what happens with time, the time derivative of $E(t)$ is always equal to 0, which implies state vector $x(t)$ always keeps inside the solution set $\Omega(t)$ of time-varying linear inequalities.

Case II If initial state $x(0) \in \mathbb{R}^n$ is outside of the initial solution set $\Omega(0)$, we obtain $g(0) > 0$. That is to say, $E(0) > 0$, from which we can conclude that $\mathrm{STP}(E(0)) = 1$, and $\dot{E}(t) = -\epsilon \Psi(E(t))$. For proving the global stability of this differential formula, it can be equivalently expressed as a set of following equations:

$$\dot{e}_i(t) = -\epsilon \Psi(e_i(t)), i = 1, 2, \cdots, n. \tag{22}$$

Define a Lyapunov function as $s_i(t) = e_i^2(t)/2 \geq 0$. Then its time derivative alongside dynamic system (22) can be computed as and its time derivative is

$$\frac{\mathrm{d}s_i(t)}{\mathrm{d}t} = -\epsilon e_i(t)\dot{e}_i(t) = -\epsilon e_i(t)\Psi(e_i(t)).$$

As proved before, AFs (12) and (14) are monotonically increasing odd functions, they satisfy $\Psi(-e_i(t)) = -\Psi(e_i(t))$, which can be written as:

$$\Psi(e_i(t)) \begin{cases} >0, & \text{if } e_i(t) > 0; \\ = 0, & \text{if } e_i(t) = 0; \\ < 0, & \text{if } e_i(t) < 0. \end{cases}$$

This property guarantees that, $\dot{s}_i(t) < 0$ is valid for $e_i(t) \neq 0$ and $\dot{s}_i(t) = 0$ only holds true for $e_i(t) = 0$. By Lyapunov stability theory [41], $e_i(t)$ globally converges to zero, when initial state $x(0) \in \mathbb{R}^n$ is outside of the initial solution set $\Omega(0)$. This means that state vector $x(t)$ converges to the theoretical solution set $\Omega(t)$ of time-varying linear inequalities in this situation.

Based on the above two cases, the proof is completed. □

3.2. Finite-time convergence

For real-time solving problems, finite-time convergence is naturally much better than infinite-time exponential convergence. In this part, we present two theorems to further prove the finite-time convergence of FTCZNN-S model (17) and FTCZNN-SL model (19), and calculate their convergence upper bounds analytically.

Theorem 2. *Given smoothly time-varying coefficient matrix* $A(t) \in \mathbb{R}^{n\times n}$ *and vector* $b(t) \in \mathbb{R}^n$, *starting from any initial state* $x(0)$, *FTCZNN-S model (17) converges to the theoretical solution set of time-varying linear inequalities in finite time. Moreover, the convergence time upper bound* T_1 *is given as follows:*

$$T_1 \leq \begin{cases} \frac{2r(L(0)^{(r-1)/2r}-1)}{\epsilon(r-1)} + \frac{2}{\epsilon(1-r)}, & L(0) \geq 1, \\ \frac{2}{\epsilon(1-r)}L(0)^{(r-1)/2}, & L(0) < 1, \end{cases} \tag{23}$$

where $L(0) = |e^+(0)|^2$ *with* $e^+(0) = \max\{|e_i(0)|\}$.

Proof. Similar to Theorem 1, the proof can also be divided into the following two cases according to different initial states $x(0)$.

Case I If initial state $x(0)$ is inside initial solution set $\Omega(0)$, we have $e_i(0) \leq 0$ and thus $\mathrm{STP}(e_i(0)) = 0$. This means that the differential formula (16) for the error function is zero. That is to say, the value of error function $E(t)$ always equals to its initial value $E(0)$ and state vector $x(t)$ remains the initial state $x(0)$, and so is the state vector $x(t)$. Thus, state solution $x(t)$ from this point is always inside the solution set. The convergence time is less than the upper bound.

Case II If initial state $x(0)$ is outside initial solution set $\Omega(0)$, we have $e_i(t) > 0$, and $\mathrm{STP}(e_i(0)) = 1$. For FTCZNN-S model (17), in this situation, its ith differential formula can be rewritten as

$$\dot{e}_i(t) = -\epsilon\Psi_1(e_i(t)), i = 1, 2, \cdots, n. \tag{24}$$

In order to calculate the upper bound, we first define an element $e^+(t)$ in Eq. (24) with $e^+(0) = \max\{|e_i(0)|\}$. Since $e_i(t)$ in Eq. (24) has the same dynamic system, according to the Comparison Lemma, we have $-|e^+(t)| \leq e_i(t) \leq |e^+(t)|$. This indicates that $e_i(t)$ converges to zero for all i when $e^+(t)$ reaches zero. Next, we calculate the convergence upper bound of $e^+(t)$ by studying the following differential system:

$$\dot{e}^+(t) = -\epsilon\Psi_1(e^+(t)).$$

Define the Lyapunov function $L(t) = |e^+(t)|^2$. The time derivative of $L(t)$ along this dynamics is computed as follows:

$$\begin{aligned} \dot{L}(t) &= 2e^+(t)\dot{e}^+(t) \\ &= -2\epsilon e^+(t)\Psi_1(e^+(t)) \\ &= -\epsilon(|e^+(t)|^{r+1} + |e^+(t)|^{\frac{1}{r}+1}) \\ &= -\epsilon(L^{\frac{r+1}{2}} + L^{\frac{r+1}{2r}}). \end{aligned} \tag{25}$$

If $L(0) \geq 1$, from the Eq. (25), we have the following inequality:

$$\dot{L} \leq -\epsilon L^{\frac{r+1}{2r}},$$

from which we can obtain

$$\mathrm{d}L \leq -\epsilon L^{\frac{r+1}{2r}}\mathrm{d}t. \tag{26}$$

Integrating both sides of the formula (26) from 0 to t, we have

$$\int_{L(0)}^{L(t)} L^{-\frac{r+1}{2r}}\,\mathrm{d}L \leq -\epsilon\int_0^t \mathrm{d}t.$$

Simplifying the inequality after integration yields to

$$L(t) \leq \left[\frac{r-1}{2r}(-\epsilon t + \frac{2r}{r-1}L(0)^{\frac{r-1}{2r}})\right]^{\frac{2r}{r-1}}.$$

Setting the left-hand side of this inequality equal to 1, we get the value of t_1:

$$t_1 = \frac{2r(L(0)^{(r-1)/2r} - 1)}{\epsilon(r-1)}$$

Thus, after time t_1, $L(t)$ decreases to 1. When $L(t) \leq 1$, the inequality Eq. (25) shows that:

$$\dot{L} \leq -\epsilon L^{\frac{r+1}{2}}.$$

Similar to solving for t_1, we compute the remaining convergence time t_2:

$$t_2 = \frac{2}{(1-r)\epsilon}$$

Hence, we obtain the convergence time upper bound $T_1 < t_1 + t_2$.

If $L(0) \leq 1$, from the Eq. (25), we have the following inequality:

$$\dot{L} \leq -\epsilon L^{\frac{r+1}{2}}, \text{ and } \mathrm{d}L \leq -\epsilon L^{\frac{r+1}{2}}\mathrm{d}t.$$

Integrating both sides of the differential inequality $\int_{L(0)}^{L(t)} L^{-\frac{r+1}{2}}\,\mathrm{d}L \leq -\epsilon\int_0^t \mathrm{d}t$, the convergence time upper bound t_3 can be computed as

$$t_3 = \frac{2}{\epsilon(1-r)}L(0)^{\frac{(1-r)}{2}}.$$

The proof is completed. □

Theorem 3. *Given smoothly time-varying coefficient matrix $A(t) \in \mathbb{R}^{n\times n}$ and vector $b(t) \in \mathbb{R}^n$, starting from any initial state $x(0)$, FTCZNN-SL model (19) converges to the theoretical solution set of time-varying linear inequalities in finite time. Moreover, the convergence time upper bound T_2 is given as follows:*

$$T_2 \leq \begin{cases} \frac{2r\ln\left[\frac{2}{L(0)^{(r-1)/2r}+1}\right]}{\epsilon(1-r)} + \frac{2\ln 2}{\epsilon(1-r)}, & L(0) \geq 1, \\ \frac{2\ln\left[1+L(0)^{(1-r)/2}\right]}{\epsilon(1-r)}, & L(0) < 1, \end{cases} \tag{27}$$

where r, ϵ, and $L(0)$ are defined as before.

Proof. Similarly, the proof is divided into the following two parts.

Case I When initial state $x(0)$ is inside the initial solution set $\Omega(0)$, the analysis is the same as Case I of Theorem 2, and is deleted due to similarity.

Case II When initial state $x(0)$ is outside the solution set $\Omega(0)$, analogous to the Case II in Theorem 2, the ith element of FTCZNN-SL model (19) can be simplified as

$$\dot{e}_i(t) = -\epsilon\Psi_2(e_i(t)).$$

Similarly, we can define $e^+(t)$ with $e^+(0) = \max\{|e_i(0)|\}$. Then, we choose the Lyapunov function $L(t) = |e^+(t)|^2$. The time derivative of $L(t)$ along this dynamics is computed as follows:

$$\begin{aligned}\dot{L} &= 2e^{+}(t)\dot{e}^{+}(t)\\ &= -2\epsilon e^{+}(t)\Psi_2(e^{+}(t))\\ &= -\epsilon(|e^{+}(t)|^{r+1} + |e^{+}(t)|^2 + |e^{+}(t)|^{\frac{1}{r}+1})\\ &= -\epsilon(L^{\frac{r+1}{2}} + L + L^{\frac{r+1}{2r}}).\end{aligned} \tag{28}$$

If $L(0)\geq 1$, considering the Eq. (28), the following inequality is satisfied:

$$\dot{L} \leq -\epsilon(L + L^{\frac{r+1}{2r}}),$$

which can be rewritten as

$$\frac{\mathrm{d}L}{L^{(r+1)/2r} + L} \leq -\epsilon \mathrm{d}t. \tag{29}$$

Integrating the formula (29) from 0 to t yields to

$$\int_{L(0)}^{L(t)} \frac{1}{L^{(r+1)/2r} + L}\,\mathrm{d}L \leq \int_0^t -\epsilon\,\mathrm{d}t,$$

which can be rewritten as follows:

$$\frac{2r}{r-1}\int_{L(0)}^{L(t)} \frac{1}{1 + L^{(r-1)/2r}}\,\mathrm{d}(L^{(r-1)/2r}) \leq \int_0^t -\epsilon\,\mathrm{d}t.$$

Let $L(t)$ equal to 1, t_4 satisfies the following equality:

$$t_4 = \frac{2r\ln\left[\frac{2}{L(0)^{(r-1)/2r}+1}\right]}{\epsilon(1-r)}.$$

When $t\geq t_4$, we have $L(t)\leq 1$. It follows from the condition (28) that

$$\dot{L} \leq -\epsilon(L^{\frac{r+1}{2}} + L). \tag{30}$$

There exists t_5 satisfying the equation:

$$t_5 = \frac{2\ln 2}{\epsilon(1-r)}.$$

The convergence time upper bound $T_2 < t_4 + t_5$.

If $L(0)\leq 1$, the inequality (30) holds and its differential form can be obtained:

$$\frac{\mathrm{d}L}{L + L^{(r+1)/2}} \leq -\epsilon \mathrm{d}t$$

Integrating both sides of the formula from 0 to t, we have:

$$\int_{L(0)}^{L(t)} \frac{1}{L + L^{(r+1)/2}}\,\mathrm{d}L \leq \int_0^t -\epsilon\,\mathrm{d}t.$$

which can be rewritten as

$$\frac{2}{1-r}\int_{L(0)}^{L(t)} \frac{1}{1 + L^{(1-r)/2}}\,\mathrm{d}(L^{(1-r)/2}) \leq \int_0^t -\epsilon\,\mathrm{d}t.$$

Thus, the convergence upper bound $T_2 < t_6$ satisfies the following equation:

$$t_6 = \frac{2\ln\left[1 + L(0)^{(1-r)/2}\right]}{\epsilon(1-r)}.$$

That completes the proof. □

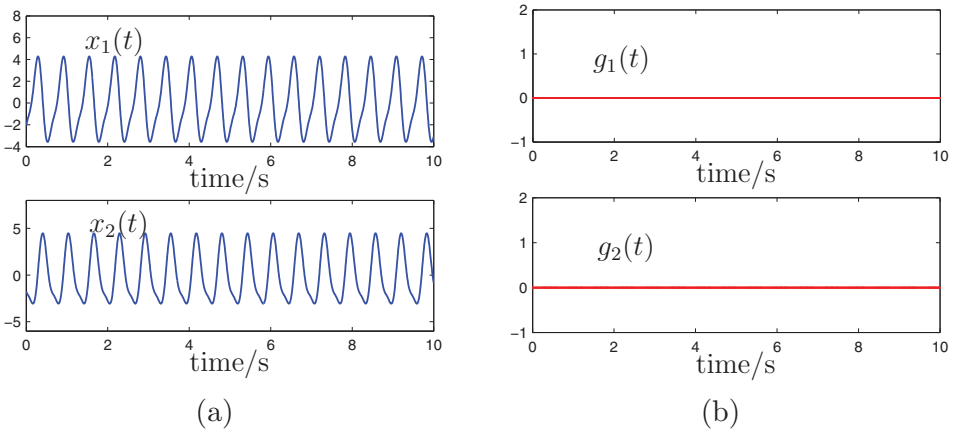

Fig. 1. Trajectories of state vector $x(t)$ and residual error $g(t)$ by applying FTCZNN-S model (17) to solve (1) when $x(0)$ is inside $\Omega(0)$ with $\epsilon = 1$ and $p = 0.3$ in Example 1. (a) Trajectories of $x(t)$. (b) Trajectories of $g(t)$.

4. Simulative verification

In this part, two illustrative computer-simulation examples are provided to evaluate the performance of FTCZNN-S model (17) and FTCZNN-SL model (19) for finding the solution of time-varying linear inequalities. Moreover, in order to provide the substantiation of the finite-time convergence performance, simulative results of FTCZNN models and ZNN model are comparatively analyzed.

Example 1. For investigation, consider time-varying linear inequality (1) with the following coefficients:

$$A(t) = \begin{bmatrix} -\sin(10t) & \cos(10t) \\ \cos(10t) & \sin(10t) \end{bmatrix}, \text{ and } b(t) = \begin{bmatrix} \sin(10t) \\ \cos(10t) \end{bmatrix}.$$

If initial state vector $x(0)$ is inside the initial solution set $\Omega(0)$, when applying FTCZNN-S model (17) to solve Example 1 with $\epsilon = 1$ and $r = 0.3$, the state trajectory can be seen from Fig. 1(a). In order to make it easier to understand, Fig. 1(b) shows the trajectory of the corresponding residual error $g(t) = A(t)x(t) - b(t)$. From it, we can obtain that residual error $g(t)$ is always equal to 0, which verifies corresponding theoretical results of this case. If initial state vector $x(0)$ is outside the initial solution set $\Omega(0)$, the trajectory of $x(t)$ can be seen from Fig. 2(a). The blue solid line shows the actual solution of Example 1 and the red one draws the upper bound of the solution set, which means that $x(t)$ effectively converges to the solution set of Example 1. Similarly, Fig. 2(b) shows the trajectory of residual error $g(t) = A(t)x(t) - b(t)$, which decreases to zero within finite time 2.5 s.

Besides, 2-norm $\|E(t)\|_2$ of the error function is used to evaluate the whole convergence performance of various ZNN models, and the corresponding results are shown in Fig. 3. As seen from this figure, FTCZNN-S model (17) and FTCZNN-SL model (19) have better convergence performance than the conventional ZNN models activated by the linear activation function (8), the power function (9), the bipolar-sigmoid function (10) and the smooth power-sigmoid function (11) [42–45]. In addition, it can be concluded that such two FTCZNN

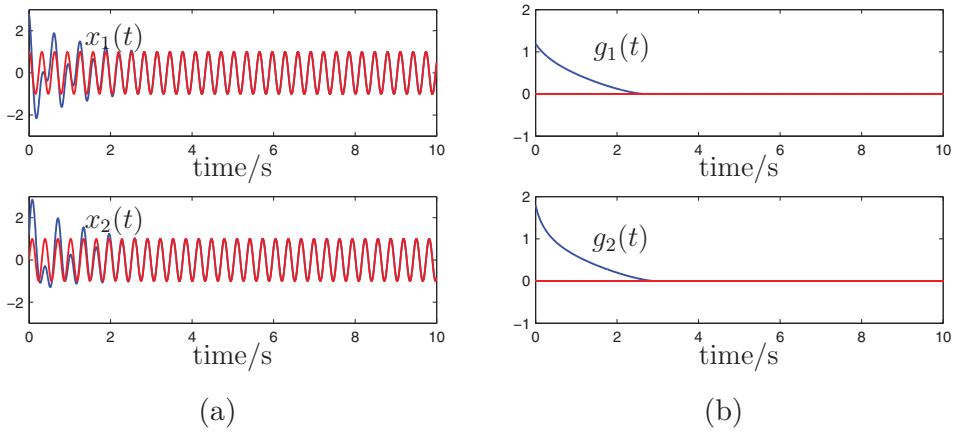

Fig. 2. The actual and theoretical trajectories of state vector $x(t)$ and residual error $g(t)$ by applying FTCZNN-S model (17) to solve (1) when $x(0)$ is outside $\Omega(0)$ with $\epsilon = 1$ and $r = 0.3$ in Example 1. (a) Trajectories of $x(t)$. (b) Trajectories of $g(t)$.

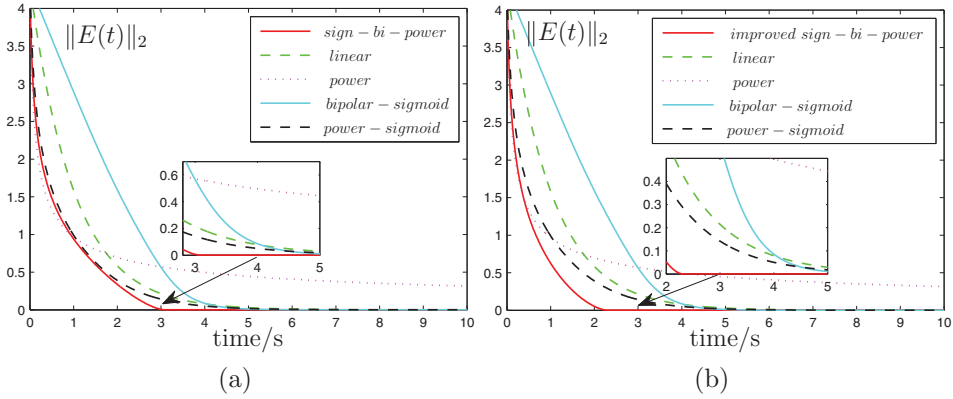

Fig. 3. Comparisons of two FTCZNN models with the conventional ZNN models activated by other AFs with $\epsilon = 1$ and $r = 0.3$ in Example 1. (a) By FTCZNN-S model (17). (b) By FTCZNN-SL model (19).

models can reach to zero within 3 s, while the conventional ZNN models have a relatively large estimation errors when $t = 3$ s. The above simulation results demonstrate the superiority of two FTCZNN models in solving time-varying linear inequalities.

In order to verify the estimation of the convergence time in Theorems 2 and 3, we choose two specific different initial states, and the following two cases are discussed.

Case I Let $x(0) = [3, 0.5]^{\mathrm{T}}$, which means that $E(0) = A(0)x(0) - b(0) = [0.5, 2]^{\mathrm{T}}$, and $L(0) = |e^{+}(0)|^2 = 2^2 = 4 > 1$. The parameters of FTCZNN-S model (17) are given as $r = 0.3$ and $\epsilon = 1$. By Theorem 2, the convergence time upper bound t_a is given as

$$t_a = \frac{2r(L(0)^{(r-1)/2r} - 1)}{\epsilon(r-1)} + \frac{2}{\epsilon(1-r)} \approx 3.5442 \text{ s}.$$

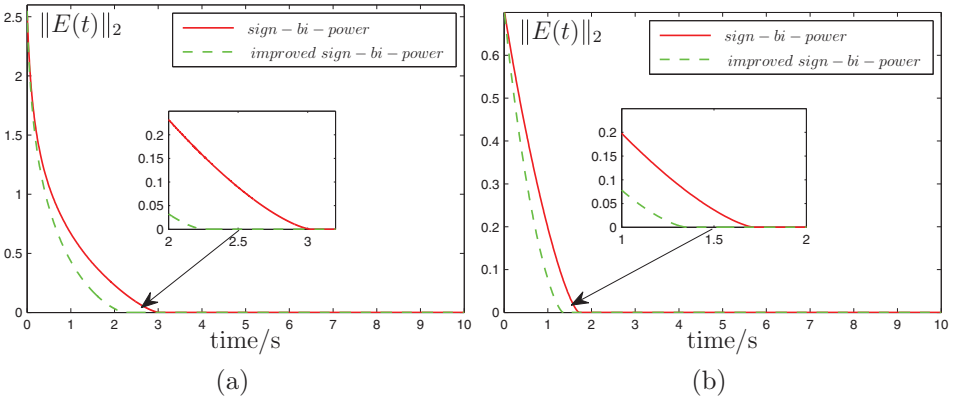

Fig. 4. Comparisons of FTCZNN-S model (17) and FTCZNN-SL model (19) with $\epsilon = 1$ and $r = 0.3$ in Example 1. (a) $L(0) > 1$. (b) $L(0) < 1$.

Let $r = 0.3$ and $\epsilon = 1$. By Theorem 3, the convergence time upper bound t_b for FTCZNN-SL model (19) is given as

$$t_b = \frac{2r \ln\left[\frac{2}{L(0)^{(r-1)/2r}+1}\right]}{\epsilon(1-r)} + \frac{2\ln 2}{\epsilon(1-r)} \approx 2.4194 \text{ s}.$$

In the situation of $L(0) \geq 1$, from the simulation results in Fig. 4(a), the actual convergence time is 3.02 s for FTCZNN-S model (17) and 2.12 s for FTCZNN-SL model (19), which are smaller than the theoretical results computed in the above.

Case II Let $x(0) = [1.5, 0.5]^{\mathrm{T}}$, which means that $E(0) = A(0)x(0) - b(0) = [0.5, 0.5]^{\mathrm{T}}$, and $L(0) = |e^{+}(0)|^2 = (0.5)^2 = 0.25 < 1$. The parameters of FTCZNN-S model (17) are given as $r = 0.3$ and $\epsilon = 1$. By Theorem 2, the convergence time upper bound t_a in this situation is computed as

$$t_a = \frac{2}{\epsilon(1-r)} L(0)^{(1-r)/2} \approx 1.7588 \text{ s}.$$

For FTCZNN-SL model (19) with the same parameters, by Theorem 3, the convergence time upper bound t_b is given as

$$t_b = \frac{2\ln\left[1 + L(0)^{(1-r)/2}\right]}{\epsilon(1-r)} \approx 1.3705 \text{ s}.$$

In this case, the simulative results are shown in Fig. 4(b), which implies the actual convergence time is also less than the theoretical upper bound of the convergence time. Specifically, the difference between the actual convergence time 3.02 s and the theoretical convergence time upper bound 3.5442 s for FTCZNN-S model (17) is larger than that between 2.12 s and 2.4194 s for FTCZNN-SL model (19). That is to say, the actual convergence time of FTCZNN-SL model (19) is much closer to the theoretical convergence time upper bound. It means that FTCZNN-SL model (19) has better convergence performance than FTCZNN-S model (17).

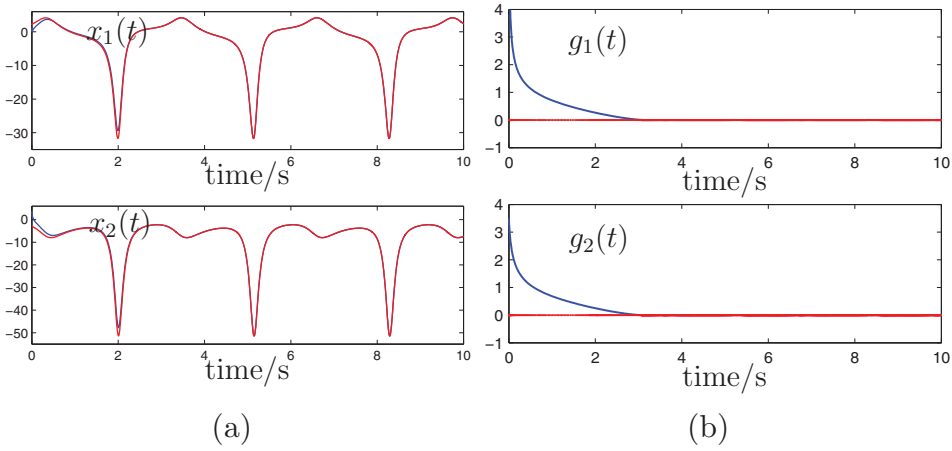

Fig. 5. The actual and theoretical trajectories of state vector $x(t)$ and residual error $g(t)$ by applying FTCZNN-S model (17) to solve (1) when $x(0)$ is outside $\Omega(0)$ with $\epsilon = 1$ and $r = 0.3$ in Example 2. (a) Trajectories of $x(t)$. (b) Trajectories of $g(t)$.

Example 2. To further verify the finite-time convergence of two FTCZNN models, we consider a different time-varying linear inequality with the following more complicated coefficients:

$$A(t) = \begin{bmatrix} 4+\sin(2t) & 3\cos(2t) \\ 3\sin(2t) & \sin(2t)\cos(2t)+1 \end{bmatrix}, \text{ and } b(t) = \begin{bmatrix} 3\sin(2t) \\ \cos(2t)-4 \end{bmatrix}.$$

As shown in Example 1, it is obvious that, when initial state $x(0)$ is inside the initial solution set $\Omega(0)$, such two FTCZNN models are stable at its initial value without iteration. Therefore, we mainly consider the situation when initial state $x(0)$ is outside the initial solution set $\Omega(0)$. As shown in Fig. 5(a), the evolvement of vector state $x(t)$ coincides with the theoretical upper bound trajectory. Moreover, Fig. 5(b) implies that the residual error can converge to zero within 2.9 s.

Besides, we also compare the proposed two FTCZNN models with existing ZNN model activated by AFs (8)-(11), with the results shown in Fig. 6. It follows that FTCZNN-S model (17) converges to zero within 3 s, and FTCZNN-SL model (19) converges to zero within 2.21 s; while the others cannot converge to zero under the same conditions.

In this example, similar to Example 1, we also select two different specific initial states and consider the following two cases.

Case I Let initial state $x(0) = [1.5, 0.5]^{\mathrm{T}}$ and the corresponding initial error function can be calculated as $E(0) = A(0)x(0) - b(0) = [7.5, 3.5]^{\mathrm{T}}$, which leads to $L(0) = |e^{+}(0)|^2 = (7.5)^2 = 56.25 > 1$. The parameters of FTCZNN-S model (17) are given as $r = 0.3$ and $\epsilon = 1$. According to Theorem 2, the convergence time upper bound t_a satisfies the following formula:

$$t_a = \frac{2r(L(0)^{(r-1)/2r} - 1)}{\epsilon(r-1)} + \frac{2}{\epsilon(1-r)} \approx 3.7065 \text{ s}.$$

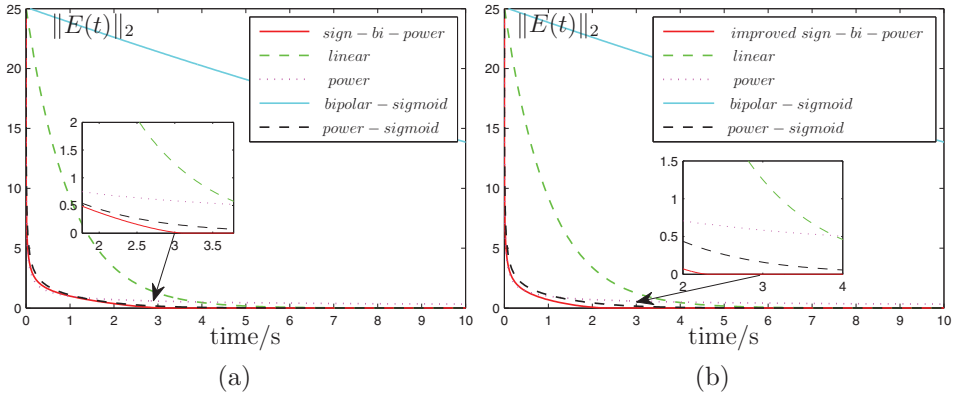

Fig. 6. Comparisons of two FTCZNN models with the conventional ZNN models activated by other AFs with $\epsilon = 1$ and $r = 0.3$ in Example 2. (a) By FTCZNN-S model (17). (b) By FTCZNN-SL model (19).

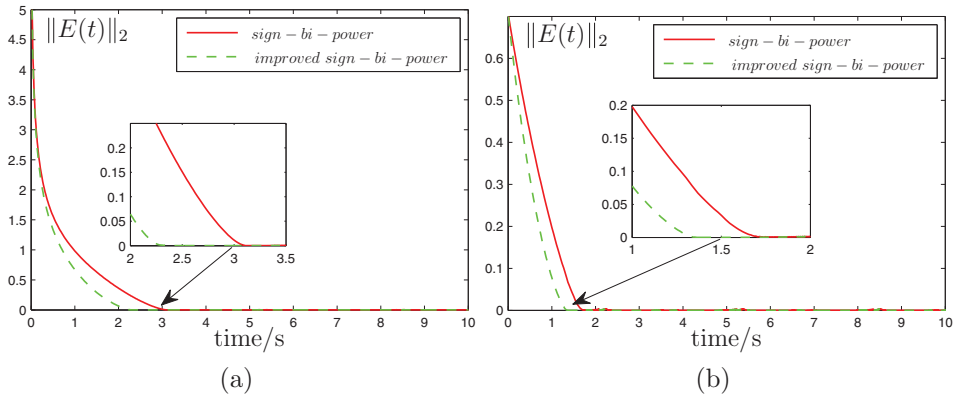

Fig. 7. Comparisons of the FTCZNN-S model (17) and FTCZNN-SL model (19) with $\epsilon = 1$ and $r = 0.3$ in Example 2. (a) when $L(0) > 1$. (b) when $L(0) < 1$.

Let $r = 0.3$ and $\epsilon = 1$, by Theorem 3, the convergence time upper bound t_b for FTCZNN-SL model (19) is given as

$$t_b = \frac{2r \ln\left[\frac{2}{L(0)^{(r-1)/2r}+1}\right]}{\epsilon(1-r)} + \frac{2\ln 2}{\epsilon(1-r)} \approx 2.5668 \text{ s}.$$

Case II Let $x(0) = [2, -2.5]^{\mathrm{T}}$, which means that $E(0) = A(0)x(0) - b(0) = [0.5, 0.5]^{\mathrm{T}}$, and $L(0) = |e^{+}(0)|^2 = (0.5)^2 = 0.25 < 1$. The parameters of FTCZNN-S model (17) are given as $r = 0.3$ and $\epsilon = 1$. Known from Theorem 2, the convergence time upper bound t_a is shown as

$$t_a = \frac{2}{\epsilon(1-r)} L(0)^{(1-r)/2} \approx 1.7588 \text{ s}.$$

While employing FTCZNN-SL model (19), by Theorem 3, the convergence time upper bound t_b in this situation is computed as follows:

$$t_b = \frac{2\ln\left[1 + L(0)^{(1-r)/2}\right]}{\epsilon(1-r)} \approx 1.3705 \text{ s}.$$

Similar to the experiment results in Example 1, from Fig. 7, we know that FTCZNN-SL model (19) has the fastest convergent rate and shortest convergence time. Moreover, it is worth mentioning that the convergence time upper bound of two FTCZNN models is only related to $L(0)$ and design parameters. Even if time-varying linear inequalities have different coefficients, they may have the same $e^{+}(t)$ and the same theoretical convergence upper bound, as shown in Case II of Examples 1 and 2.

5. Conclusions

In this paper, by exploring two novel nonlinear AFs, two FTCZNN models have been proposed to solve the time-varying linear inequalities. Since design formulas fully consider the time derivative information of time-varying coefficients, two FTCZNN models are theoretically proved to be globally convergent when applied to solve time-varying linear inequalities. Furthermore, the proposed two FTCZNN models have been proved to possess the finite-time convergence with the corresponding upper bounds estimated. At last, two numerical simulation examples have been presented to validate the great properties of two FTCZNN models by comparing the conventional ZNN model activated by the linear AF, the power AF, the bipolar-sigmoid AF, and the power-sigmoid AF.

Acknowlgedgments

This work was supported by the National Natural Science Foundation of China under grants 61866013, 61976089, and 61966014; the Natural Science Foundation of Hunan Province of China under grants 2019JJ50478, and 18A289; and the Hunan Provincial Science and Technology Project Foundation of China under grants 2018TP1018, and 2018RS3065.

References

[1] Y. Zhang, B. Cai, L. Zhang, K. Li, Bi-criteria velocity minimization of robot manipulators using a linear variational inequalities-based primalcdual neural network and puma 560 example, Adv. Robot. 22 (13–14) (2008) 1479–1496.
[2] C.K. Ahn, Linear matrix inequality optimization approach to exponential robust filtering for switched Hopfield neural networks, J. Optim. Theory Appl. 154 (2) (2012) 573–587.
[3] X. Liang, S.K. Tso, An improved upper bound on step-size parameters of discrete-time recurrent neural networks for linear inequality and equation system, IEEE Trans. Circuits Syst. 49 (5) (2002) 695–698.
[4] F. Hao, X. Zhao, Linear matrix inequality approach to static outputfeedback stabilisation of discrete-time networked control systems, Control Theory Appl. IET 4 (7) (2010) 1211–1221.
[5] T. Su, C. Wei, S. Huang, et al., Image noise cancellation using linear matrix inequality and cellular neural network, Opt. Commun. 281 (23) (2008) 5706–5712.
[6] G. Labonte, On solving systems of linear inequalities with artificial neural networks, IEEE Trans. Neural Netw. 8 (3) (1997) 590–600.
[7] C. Lin, C. Lai, T. Huang, A neural network for linear matrix inequality problems, IEEE Trans. Neural Netw. 11 (5) (2000) 1078–1092.
[8] D. Guo, Y. Zhang, Zhang neural network for online solution of time-varying linear matrix inequality aided with an equality conversion, IEEE Trans. Neural Netw. Learn. Syst. 25 (2) (2014) 370–382.

[9] K. Yang, K.G. Murty, O.L. Mangasarian, New iterative methods for linear inequalities, J. Optim. Theory Appl. 72 (1) (1992) 163–185.
[10] S. Qin, X. Xue, A two-layer recurrent neural network for nonsmooth convex optimization problems, IEEE Trans. Neural Netw. 26 (6) (2015) 1149–1160.
[11] S. Qin, X. Le, J. Wang, A neurodynamic optimization approach to bilevel quadratic programming, IEEE Trans. Neural Netw. Learn. Syst. 28 (11) (2017) 2580–2591.
[12] L. Xiao, B. Liao, S. Li, Design and analysis of FTZNN applied to real-time solution of nonstationary Lyapunov equation and tracking control of wheeled mobile manipulator, IEEE Trans. Ind. Inform. 14 (1) (2018) 98–105.
[13] S. Qin, J. Feng, J. Song, et al., A one-layer recurrent neural network for constrained complex-variable convex optimization, IEEE Trans. Neural Netw. Learn. Syst. 29 (3) (2018) 534–544.
[14] N. Liu, S. Qin, A neurodynamic approach to nonlinear optimization problems with affine equality and convex inequality constraints, Neural Netw. 109 (2019) 147–158.
[15] W. Jia, S. Qin, X. Xue, A generalized neural network for distributed nonsmooth optimization with inequality constraint, Neural Netw. 119 (2019) 46–56.
[16] X. Hu, J. Wang, Design of general projection neural networks for solving monotone linear variational inequalities and linear and quadratic optimization problems, IEEE Trans. Syst. Man Cybern. B, Cybern. 37 (5) (2007) 1414–1421.
[17] H. Wu, R. Shi, L. Qin, et al., A nonlinear projection neural network for solving interval quadratic programming problems and its stability analysis, Math. Probl. Eng. 2010 (2010) 1–13.
[18] A.Y. Alanis, E.N. Sanchez, A.G. Loukianov, et al., Discrete-time recurrent high order neural networks for nonlinear identification, J. Frankl. Inst. 347 (7) (2010) 1253–1265.
[19] F.O. Tellez, A.G. Loukianov, E.N. Sanchez, et al., Decentralized neural identification and control for uncertain nonlinear systems: application to planar robot, J. Frankl. Inst. 347 (6) (2010) 1015–1034.
[20] Y. Xia, J. Wang, D. Hung, Recurrent neural networks for solving linear inequalities and equations, IEEE Trans. Circuits Syst. I 46 (1999) 452–462.
[21] X. He, T. Huang, C. Li, et al., A recurrent neural network for optimal real-time price in smart grid, Neurocomputing 149 (2015) 608–612.
[22] L. Xiao, Y. Zhang, Zhang neural network versus gradient neural network for solving time-varying linear inequalities, IEEE Trans. Neural Netw. 22 (10) (2011) 1676–1684.
[23] L. Xiao, Y. Zhang, Different Zhang functions resulting in different ZNN models demonstrated via time-varying linear matrix-vector inequalities solving, Neurocomputing 121 (2013) 140–149.
[24] Y. Zhang, W. Ma, B. Cai, From Zhang neural networks to newton iteration for matrix inversion, IEEE Trans. Circuits Syst. I 56 (2009) 1405–1415.
[25] D. Guo, Y. Zhang, A new variant of Zhang neural network for solving online time-varying linear inequalities, Proc. R. Soc. A 468 (2144) (2012) 2255–2271.
[26] L. Xiao, Accelerating a recurrent neural network to finite-time convergence using a new design formula and its application to time-varying matrix square root, J. Frankl. Inst. 354 (13) (2017) 5667–5677.
[27] S. Li, S. Chen, B. Liu, Accelerating a recurrent neural network to finite-time convergence for solving time–varying sylvester equation by using a sign-bi-power activation function, Neural Process. Lett. 37 (2) (2013) 189–205.
[28] Y. Shen, P. Miao, Y. Huang, et al., Finite-time stability and its application for solving time-varying Sylvester equation by recurrent neural network, Neural Process. Lett. 42 (3) (2015) 763–784.
[29] S.G. Nersesov, W.M. Haddad, Q. Hui, Finite-time stabilization of nonlinear dynamical systems via control vector Lyapunov functions, J. Frankl. Inst. 345 (7) (2008) 819–837.
[30] J. Jin, L. Xiao, M. Lu, J. li, Design and analysis of two FTRNN models with application to time-varying sylvester equation, IEEE Access 7 (2019a) 58945–58950.
[31] J. Jin, L. Zhao, M. Li, et al., Improved zeroing neural networks for finite time solving nonlinear equations, Neural Comput. Appl. 29 (2019b).
[32] H. Liu, T. Zhang, Neural network-based robust finite-time control for robotic manipulators considering actuator dynamics, Pergamon Press, Inc., 2013.
[33] S. Hou, J. Fei, C. Chen, Y. Chu, Finite-time adaptive fuzzy neural network control of active power filter, IEEE Trans. Power Electr. 34 (10) (2019) 10298–10313.
[34] A. Zou, K. Kumar, Z. Hou, X. Liu, Finite-time attitude tracking control for spacecraft using terminal sliding mode and Chebyshev neural network, IEEE Trans. Syst., Man, Cybern. B 41 (4) (2011) 950–963.
[35] N. Zhou, R. Chen, Y. Xia, et al., Neural network-based reconfiguration control for spacecraft formation in

obstacle environments: neural network-based reconfiguration control for spacecraft formation, Int. J. Robust Nonlin. 28 (7) (2018) 2442–2456.

[36] F. Xu, Z. Li, Z. Nie, et al., Zeroing neural network for solving time-varying linear equation and inequality systems, IEEE Trans. Neural Netw. Learn. Syst. 30 (8) (2019) 2346–2357.

[37] L. Jin, S. Li, Nonconvex function activated zeroing neural network models for dynamic quadratic programming subject to equality and inequality constraints, Neurocomputing 267 (6) (2017) 107–113.

[38] L. Xiao, S. Ding, M. Mao, et al., Finite-time convergence analysis and verification of improved ZNN for real-time matrix inversion, in: Proceedings of the IEEE International Conference on Information Science and Technology, 2014, pp. 26–28.

[39] Y. Zhang, B. Qiu, L. Jin, et al., Infinitely many Zhang functions resulting in various ZNN models for time–varying matrix inversion with link to drazin inverse, Informat. Process. Lett. 115 (9) (2015) 703–706.

[40] L. Xiao, Z. Zhang, et al., Design, verification and robotic application of a novel recurrent neural network for computing dynamic sylvester equation, Neural Netw. 105 (2018) 185–196.

[41] L. Xiao, Y. Zhang, et al., Performance benefits of robust nonlinear zeroing neural network for finding accurate solution of Lyapunov equation in presence of various noises, IEEE Trans. Ind. Informat. 15 (9) (2019) 5161–5171.

[42] Y. Zhang, S.S. Ge, Design and analysis of a general recurrent neural network model for time-varying matrix inversion, IEEE Trans. Neural Netw. 16 (6) (2005) 1477–1490.

[43] L. Xiao, Y. Zhang, et al., A noise tolerant zeroing neural network for time-dependent complex matrix inversion under various kinds of noises, IEEE Trans. Ind. Informat. (2019a).

[44] L. Xiao, Y. Zhang, et al., A new noise-tolerant and predefined-time ZNN model for time-dependent matrix inversion, Neural Netw. 117 (2019b) 124–134.

[45] Y. Zhang, C. Yi, D. Guo, et al., Comparison on gradient-based neural dynamics and Zhang neural dynamics for online solution of nonlinear equations, Neural Comput. Appl. 20 (1) (2011) 1–7.